



Supplement of

The contribution of oceanic halocarbons to marine and free tropospheric air over the tropical West Pacific

Steffen Fuhlbrügge et al.

Correspondence to: Kirstin Krüger (kirstin.krueger@geo.uio.no)

The copyright of individual parts of the supplement might differ from the CC-BY 3.0 licence.

1 **Supplement**

3 **Convective energy and precipitation**

4 Intense solar insolation and high sea surface temperatures (SST) favour the South China and
5 Sulu Seas for high convective activity. To indicate atmospheric instabilities that can lead to
6 convective events the convective available potential energy (*CAPE*) (Margules, 1905;
7 Moncrieff and Miller, 1976) is calculated. *CAPE* is defined as the cumulative buoyant energy
8 of an air parcel from the level of free convection (*LFC*), the level where the environmental
9 temperature decreases faster than the moist adiabatic lapse rate of a saturated air parcel at the
10 same level, and the equilibrium level (*EL*), the height at which the air parcel has the same
11 temperature as the environment. *CAPE* is computed after S-Eq. 1, with g as the gravitational
12 constant, $T_{v,p}$ as the virtual temperature of an adiabatic ascending air parcel at geometric
13 height z , $T_{v,e}$ as the virtual temperature of the environment at z , z_{LFC} as the height of the level
14 of free convection and z_{EL} as the height of the equilibrium level. *CAPE* can range from 0 to
15 more than 3 kJ/kg for very intense thunderstorms (Thompson and Edwards, 2000).

16

$$CAPE = \int_{z_{LFC}}^{z_{EL}} g \cdot \left(\frac{T_{v,p} - T_{v,e}}{T_{v,e}} \right) dz \quad (\text{S-Eq. 1})$$

17

18 The mean CAPE computed from the radiosonde data is $998 \pm 630 \text{ Jkg}^{-1}$ and typically
19 elevated for tropical regions (S-Figure 1). Highest CAPE during the cruise was observed on
20 November 16, 2011 at 12 UTC in the southern South China Sea and exceeded 2.9 kJkg^{-1} ,
21 revealing developing convection. ERA-Interim mean CAPE during the cruise was 825 ± 488
22 Jkg^{-1} and about 170 Jkg^{-1} lower than observed by the radiosondes.

23 Precipitation measurements by the optical disdrometer ODM-470 are shown in S-Figure 1.
24 Besides a number of small rain events during the cruise, three major convective rain events
25 are evident on November 16, 21 and 24, 2011. The total amount of accumulated rain during
26 the cruise was 52.3 mm. The most intense rain rate of 16.3 mmh^{-1} was observed on
27 November 16, 2011 in the southwest South China Sea. The relatively low total precipitation
28 during the cruise is reflected by negative precipitation anomalies in November 2011
29 compared to the long term climate mean along the northern coast of Borneo (Climate
30 Diagnostics Bulletin, November 2011, Climate Prediction Center).

32 **R/V SONNE – R/A FALCON: Identifying observations of the same air mass**
33 To investigate if the same air masses were observed on R/V SONNE and on R/A FALCON a
34 perfluorocarbon tracer was released on R/V SONNE on November 21, 2011, which was
35 indeed detected 25 hours later on R/A FALCON (Ren et al., 2014). With the trajectory
36 calculations it can be determined which fraction of the air masses investigated on R/V
37 SONNE could subsequently be investigated on R/A FALCON. Within a horizontal distance
38 of ± 20 km and a maximum vertical distance of ± 1 km around the position of the aircraft, as
39 well as a time frame of ± 3 hrs of the VSLS air measurements on R/A FALCON, 15 % of all
40 launched $80 \times 10,000$ surface trajectories, marking the air masses on R/V SONNE, passed the
41 R/A FALCON flight track during the cruise. The amount of trajectories passing the flight
42 track of R/A FALCON increases to 77 ± 29 % between November 16 and December 11,
43 2011 within a time frame of up to 10 days.

44

45

46 **References**

47 Margules, M.: Über die Energie der Stürme. K. k. Zentralanstalt für Meteorologie und
48 Erdmagnetismus in Wien, 1905.

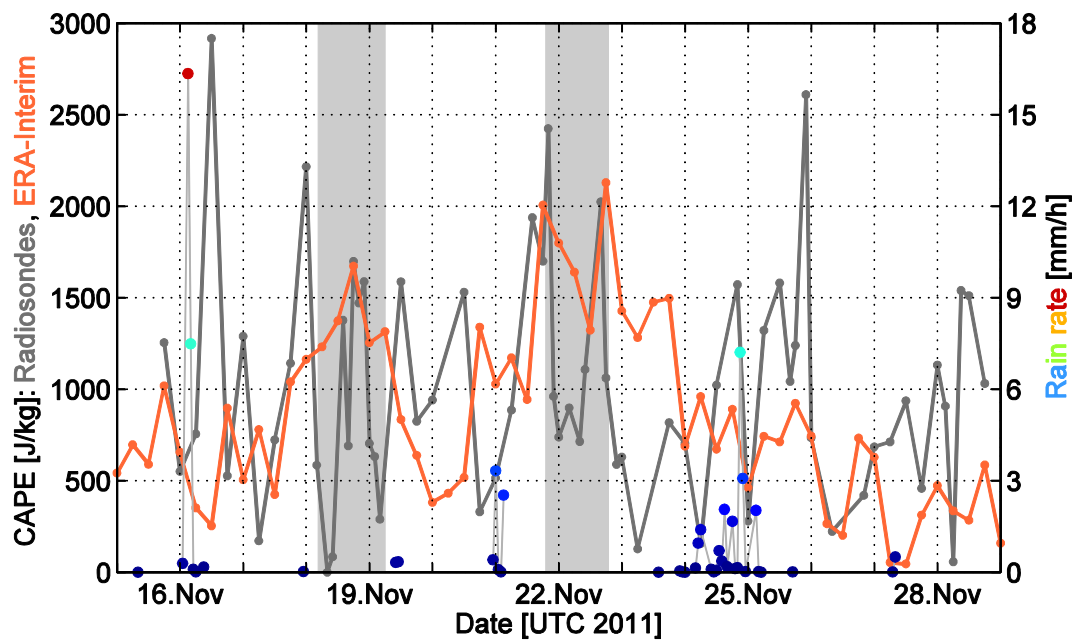
49 Moncrieff, M. and Miller, M.: Dynamics and simulation of tropical cumulonimbus and squall
50 lines, Quarterly Journal of the Royal Meteorological Society, 102, 373-394, 1976.

51 Ren, Y., Baumann, R., and Schlager, H.: An airborne perfluorocarbon tracer system and its
52 first application for a Lagrangian experiment, 7, 6791-6822, 2014.

53 Thompson, R. and Edwards, R.: An overview of environmental conditions and forecast
54 implications of the 3 May 1999 tornado outbreak, Weather and Forecasting, 15, 682-699,
55 2000.

56

57



60 **S-Figure 1:** Left scale: convective available potential energy (CAPE) from
 61 radiosondes on R/V SONNE (grey) and ERA-Interim (orange). Right scale: Rain rate
 62 (colored dots) during the cruise, observed by an optical disdrometer (ODM 470) on R/V SONNE. The two shaded
 63 areas (light grey) in the background show the 24 h stations.

S-Table 1: As Table 3 and Table 4 using ERA-Interim MABL height.

	OD [% day ⁻¹]	COL [% day ⁻¹]	CL [% day ⁻¹]	AD [% day ⁻¹]	ODR	CLR	ADR	VMR _{ODR} [ppt]	VMR _{CLR} [ppt]	VMR _{ADR} [ppt]	MABL-FT Flux [pmol m ⁻² hr ⁻¹]
CHBr₃	87.0 ±	-224.9 ±	-7.1	144.9 ±	0.43 ±	-0.03 ±	0.60 ±	0.88 ±	-0.07 ±	1.22 ±	4251 ±
	124.5	70.7		143.1	0.56	0.01	0.55	1.18	0.04	1.20	1907
CH₂Br₂	39.3 ±	-224.9 ±	-1.2	186.7 ±	0.20 ±	-0.01 ±	0.80 ±	0.24 ±	-0.01 ±	0.93 ±	2456 ±
	40.3	70.7		83.2	0.21	0.00	0.21	0.26	0.00	0.27	921
CH₃I	135.2 ±	-224.9 ±	-24.0	113.8 ±	0.73 ±	-0.12 ±	0.39 ±	0.28 ±	-0.05 ±	0.14 ±	799 ±
	195.0	70.7		220.8	1.06	0.05	1.04	0.39	0.02	0.37	356